

Axially excited spatial double pendulum nonlinear dynamics (BIF306-15)

Michał Ludwicki, Grzegorz Kudra, Jan Awrejcewicz

Abstract: Analysis of a 3D spatial double physical pendulum system, coupled by two universal joints is performed. External excitation of the mechanism is realized by axial periodic rotations of the first joint of the pendulum. System of ODEs is solved numerically and obtained data are analyzed by a standard approach, including time series, phase plots and Poincaré sections. Additionally, FFT (Fast Fourier Transform and the wavelet transformation algorithms have been applied. Various wavelet basic functions have been compared to find the best fit, e.g. Morlet, Mexican Hat and Gabor wavelets. The so far obtained results allowed for detection of a number of non-linear effects, including chaos, quasi-periodic and periodic dynamics, as well the numerous and different bifurcations. Scenarios of transition from regular to chaotic dynamics have been also illustrated and studied.

1. Introduction

This paper presents the model and its numerical simulations of a simple 3D double physical pendulums, under variable axial excitations. The periodic torque in axial direction is the only external force considered and realized as a variable angular velocity of the pivot point of first pendulum. Damping force in each joint is modeled by introduction of linear damping characteristic.

Following the subject of current scientific publications related to the multiple physical pendulum use and analysis one can say that it deals mainly with simplified constructions having specific configurations. When searching for the available papers with regard to the pendulum model presented here, we have not detected those considering a double pendulum as a system of rigid bodies, where the only excitation source has been associated with axial vibrations.

Many papers aimed on investigations of the spatial pendulums mostly deal with the single spherical pendulum and its variants, e.g. using a single rigid body cylinder model [1–3] or using simple mathematical pendulum in space ([4], [5]).

More complex spatial pendulum configurations are studied as an objects of nonlinear analysis, but rather to test or develop a control and stabilization techniques, e.g. general model of inverted multiple mathematical pendulum control using single torque [6] or a moving cart [7] or inverted

double rigid body pendulum being the most similar to the construction presented in our paper but controlled by four external torques [8].

Another wide area of application of the pendulum models deals with damping and stabilization phenomena. However here also one can find no spatial multibody pendulums, but rather simplified mathematical pendulums, like a double mathematic pendulum model [9].

Lastly, multiple physical pendulums, often very complex, are sometimes used for modeling biological systems, especially human limbs. One can see the natural similarity of these two (bio-) mechanical systems. Unfortunately, in this scientific research pendulums are mainly used to map real body movements, so the main goal is to develop a proper control algorithm, e.g. inverted pendulum models of human gait [10] or to model some body characteristic by similar configuration of pendulums, like kicking power calculated by a similar model of a double physical pendulum [11].

Some additional vibration analysis techniques, like *Continuous Wavelets Analysis* are also presented in our paper. This investigation method is widely used in mechanical vibration analysis, including chaotic dynamics of beams [12], gears and bearings fault detection methods ([13], [14]), carrying out stability analysis during earth-quakes [15] or even brain oscillations effects using EEG and wavelets [16].

This paper presents the results of numerical computations of a complex mechanical system using both classical and non-classical (wavelets) techniques. A lot of nonlinear behavior effects of the system is observed and discussed, using multiple graphical interpretation.

1.1. The Pendulum Model

Presented mechanical system consists of two simple physical pendulums connected by two universal joints O_1 and O_2 (see Figure 1). Each single pendulum is treated as a rigid body having a mass m_i and moment of inertia approximated by an axially symmetric cylinder. Its length L_i and the position of center of masses e_i are also known. The suspension joint of first pendulum can oscillate in two directions (φ_1 and θ_1) and additionally it rotates around vertical axis with variable in time angular velocity.

The model takes into account a simple viscous damping characteristics in each joint described by the following equations:

$$\mathbf{M}_d = [M_{d\theta_1} - M_{d\theta_2}, M_{d\varphi_1} - M_{d\varphi_2}, M_{d\theta_2} - M_{d\varphi_2}]^T, \quad (1)$$

where \mathbf{M}_i are corresponding damping torques proportional to the angular velocities.

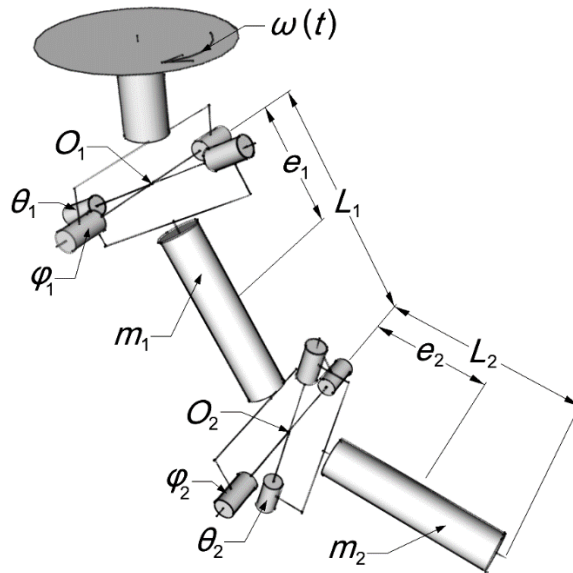


Figure 1. Coupled pendulums.

Air resistance forces have been neglected owing to their small values comparing to the mass and inertia forces occurring in the system. External source of exciting torque is applied to the point of suspension of the pendulum as a variable angular velocity function

$$\omega(t) = \omega_0 + q \sin(\Omega t), \quad (2)$$

where ω_0 is a constant part of velocity [rad/s], q states for the amplitude [N·m] and Ω stands for frequency [rad/s].

Finding potential and kinetic energy of the system and using the Langrange equations of the second kind, the governing equations of motion have been derived in an analytical way. After performing several transformations to simplify their form, a set of four ODEs can be written as follows

$$\mathbf{M}(\mathbf{q}) \cdot \begin{bmatrix} \ddot{\theta}_1 \\ \ddot{\phi}_1 \\ \ddot{\theta}_2 \\ \ddot{\phi}_2 \end{bmatrix} + \mathbf{A} \begin{pmatrix} \theta_1 \\ \phi_1 \\ \theta_2 \\ \phi_2 \end{pmatrix} \cdot \mathbf{a} + \mathbf{B} \begin{pmatrix} \theta_1 \\ \phi_1 \\ \theta_2 \\ \phi_2 \end{pmatrix} \cdot \begin{bmatrix} \dot{\theta}_1 \\ \dot{\phi}_1 \\ \dot{\theta}_2 \\ \dot{\phi}_2 \end{bmatrix} + \mathbf{R} \begin{pmatrix} \theta_1 \\ \phi_1 \\ \theta_2 \\ \phi_2 \end{pmatrix} = 0, \quad (3)$$

where $\mathbf{a} = [\dot{\theta}_1^2, \dot{\phi}_1^2, \dot{\theta}_2^2, \dot{\phi}_2^2, \dot{\theta}_1\dot{\phi}_1, \dot{\theta}_1\dot{\phi}_2, \dot{\theta}_2\dot{\phi}_1, \dot{\theta}_2\dot{\phi}_2, \dot{\phi}_1\dot{\phi}_2, \dot{\theta}_1\dot{\theta}_2]^T$ and \mathbf{M} , \mathbf{A} , \mathbf{B} , \mathbf{R} denote matrices and vectors, here not defined explicitly (see Appendix).

2. Numerical computations

Results of the numerical computations presented in this paper concern the following fixed parameters (see Fig. 1) listed in Table 1.

Table 1 Numerical computation parameters.

	simulation example	
	first joint	second joint
weight of the pendulums [kg]	$m_1 = 0.5$	$m_2 = 0.5$
length [m]	$L_1 = 0.2$	$L_2 = 0.2$
position of the mass center [m]	$e_1 = 0.1$	$e_2 = 0.1$
moments of inertia [kg·m ²]	$I_{x1} = 0.002$ $I_{y1} = 0.002$ $I_{z1} = 0.0001$	$I_{x2} = 0.002$ $I_{y2} = 0.002$ $I_{z2} = 0.0001$
viscous damping coefficient [N·s/m]	$c_1 = 0.1$	$c_2 = 0.1$

The ODEs solving algorithm (named **NDSolve** [] in *Wolfram Mathematica*® package) is based on higher order *Runge-Kutta* methods including automatic step control technique and other computation performance improvements. Numerical results are automatically interpolated to any chosen time step.

During numerical calculations, every first 400 s time steps were ignored as transient motions and next 400 or more (if needed) were used as significant for the further analysis.

2.1. The Wavelet Analysis

Numerically computed results have been studied by a standard approach, including time series, phase plots and Poincaré sections. Additionally, FFT (Fast Fourier Transform) and the wavelet transformation algorithms have been used.

Various wavelet basic functions have been compared to find the best fit, e.g. Morlet, Mexican Hat and Gabor wavelets. Detailed comparison showed that non-orthogonal Morlet wavelets [17] (see equation (4)) are the most convenient for analysis of the studied mechanical system. The *Continuous Wavelet Transformation* performed for this wavelets produces smooth wavelet scalograms with clearly exhibited frequency variations keeping relatively fast numerical calculations. This transformation is based on the following formula

$$\psi(t) = 1/\sqrt[4]{\pi} \cos(t \pi \sqrt{2/\log(2)}) \exp(-\frac{t^2}{2}) \quad (4)$$

3. Results

Here, a few representative results of classical nonlinear dynamics analysis combined with FFT and wavelet continuous transformation are presented. All plots and diagrams have been generated using *Mathematica*® package. It is important to mention, that there are three possible control parameters that control a value of angular velocity function (see eq. (2)) – a constant part of angular velocity ω_0 [rad/s], the amplitude q [N·m] and the excitation angular velocity frequency Ω [rad/s]. The periods number maps have been calculated for a constant q and variable ω_0 and Ω while bifurcation diagrams for variable control parameter Ω and constant q and ω_0 are constructed.

3.1. Classical analysis vs. Continuous Wavelets Transformation

For $\omega_0 = 6.5$ rad/s, $q = 3$ N·m, $\Omega = 6$ rad/s and very small initial deflection of the first pendulum ($\theta_1 = 0.001$ rad) the dynamical system finally tends to a stable quasi-periodic solution. The quasi-periodic pulsation can be seen clearly in the phase plot shown in Figure 2b. For this case of non-stationary nonlinear behavior, one can see an obvious advantage of the wavelet analysis, since the resulting scalograms show a structure of scale variable of wavelet basic function corresponding to frequency vs. time.

The dark horizontal line in the wavelet scalogram (Figure 2d) on scale level 5 represents the quasi-periodic solution (after $t \approx 300$ s), while the dark regions in higher scales (before $t \approx 300$ s) correspond to the transient behavior. In general, in wavelet analysis, the higher the scale value is a lower frequency is represented. Similar observation holds for a 3D representation of this scalogram reported in Figure 2e.

For higher amplitude of excitation $q = 12$ N·m, keeping constant $\omega_0 = 0$ rad/s and $\Omega = 5.49$ rad/s our dynamical system exhibits chaotic behavior. It can be seen in the Poincaré sections in Figure 3a and the in the phase plots in Figure 3b. The FFT analysis distinguishes one outstanding frequency which is also seen in the wavelet scalogram marked by one darker horizontal region on scale level 3.

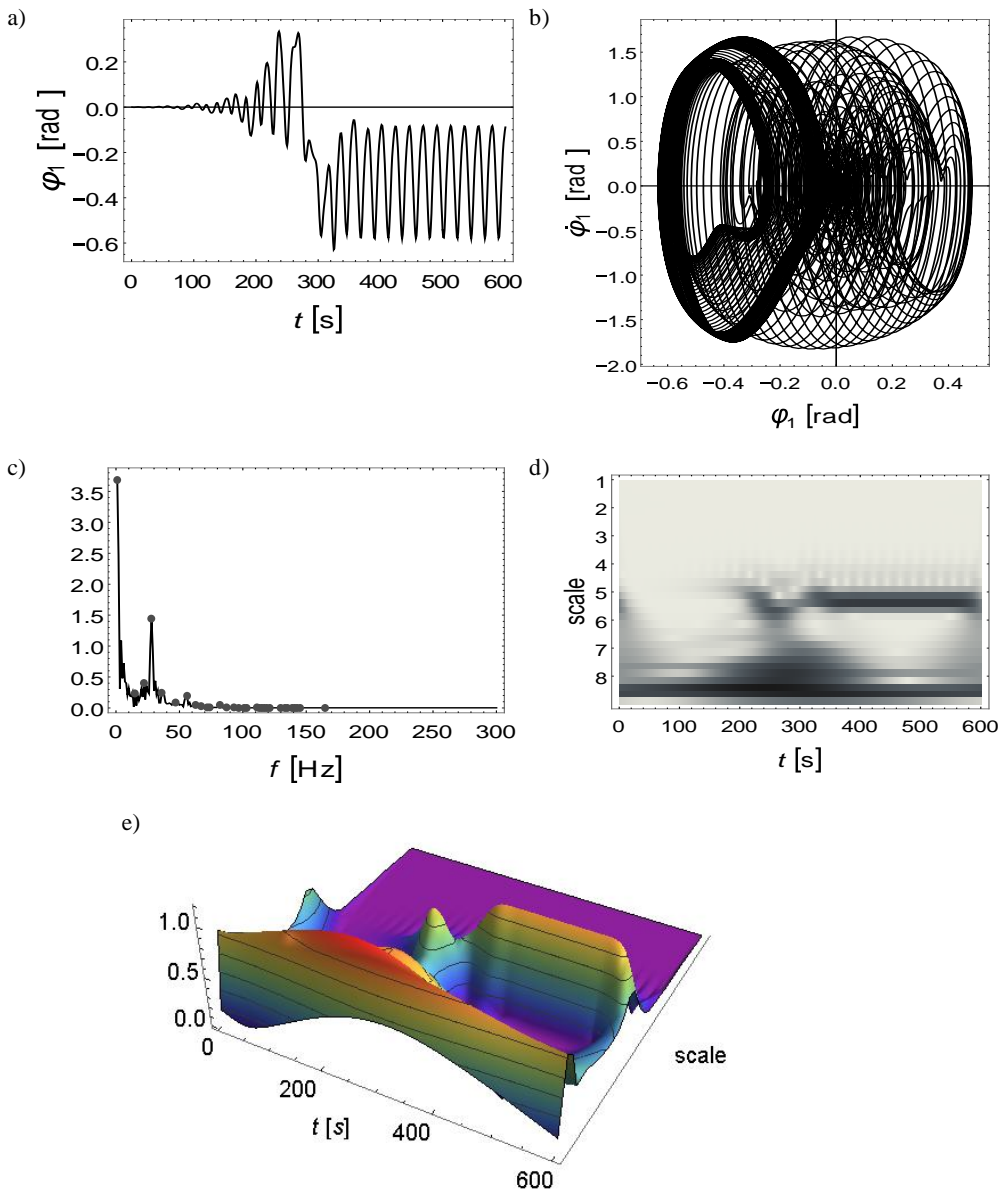


Figure 2. Time series (a), phase plots (b), FFT analysis (c), wavelets scalogram (d) and the same scalogram in 3D (e) for $\omega_0 = 6.5$ rad/s, $q = 3$ N·m, $\Omega = 6$ rad/s.

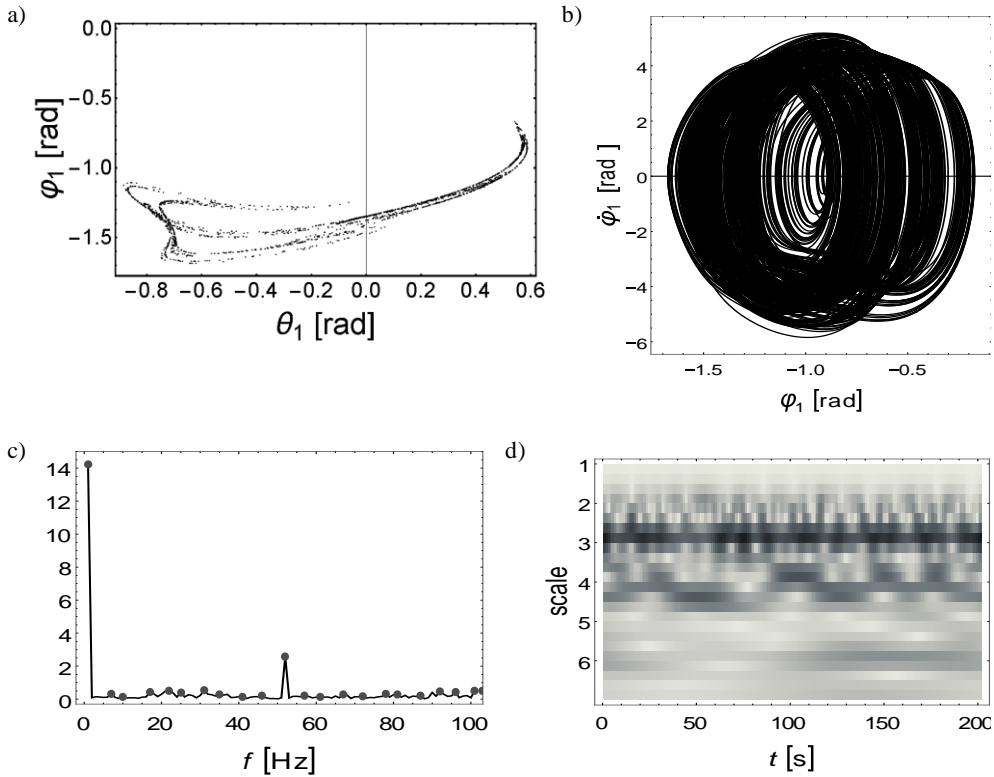


Figure 3. Poincaré section for 2000 s (a), phase plots (b), FFT analysis (c) and wavelets scalogram (d) for 200 s ($\omega_0 = 0$ rad/s, $q = 12$ N·m, $\Omega = 5.49$ rad/s).

Last set of the presented results (see Figure 4) contains maps showing a number of periods, which are combined with bifurcational diagrams for three different amplitudes of excitation. The white horizontal line in the maps shows the path of control parameter changes in corresponding bifurcational diagrams. The gray background of the maps represents one period vibrations, while the dark regions, a maximum counted periods, which corresponds to chaos or a high-order quasi-periodicity.

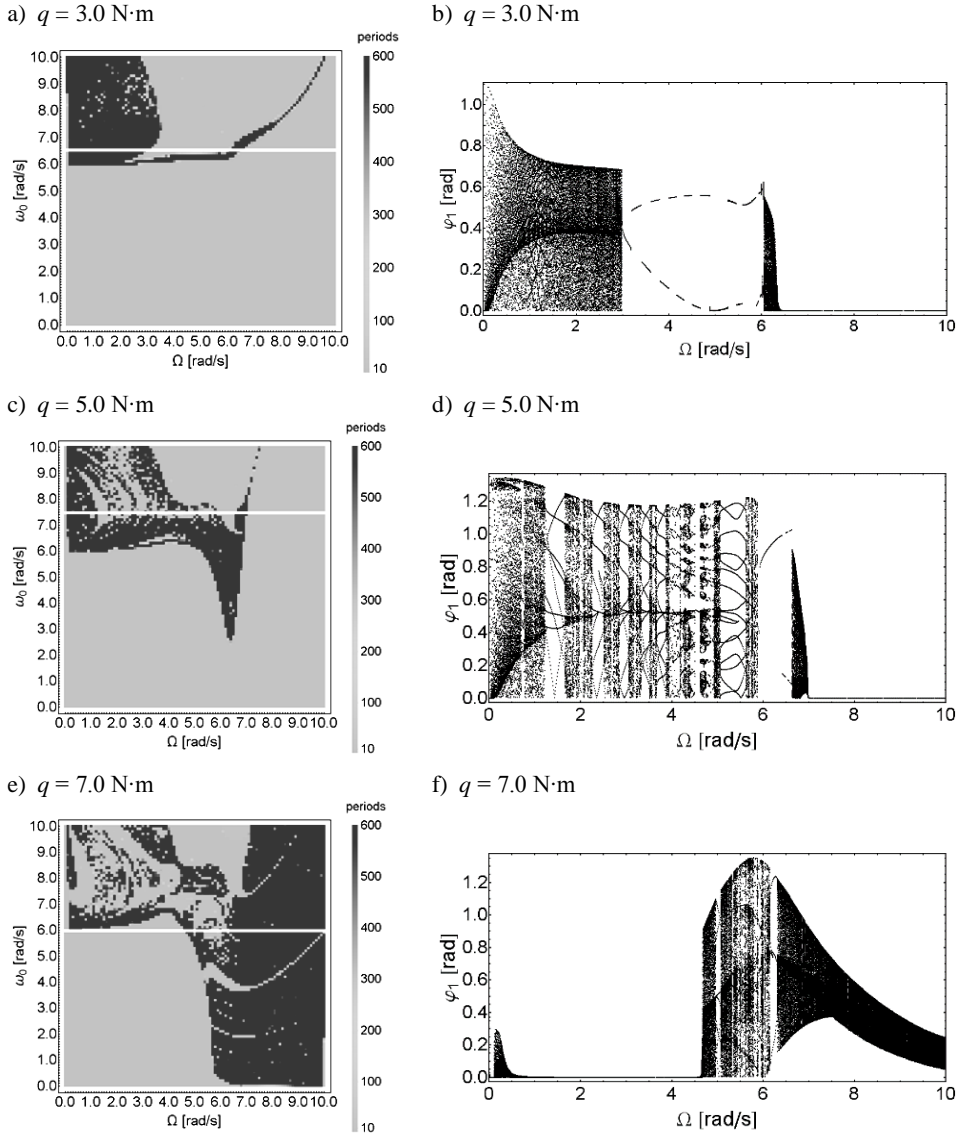


Figure 4. Periods number in the plane (ω_0, Ω) for constant amplitude q , after 400 s of transient oscillations and bifurcation diagrams for φ_1 with variable Ω and constant value of ω_0 marked by white horizontal line on the maps. (a)-(b) for $q = 3 \text{ N}\cdot\text{m}$, (c)-(d) for $q = 5 \text{ N}\cdot\text{m}$ and (e)-(f) for $q = 7 \text{ N}\cdot\text{m}$.

Observe that both charts presented in pairs in Figure 4, are complementary. The knowledge of the number of periods provides a general information of the nature of system dynamical behaviour, while bifurcational diagrams supply more complex data, but for a particular range of the control

parameter. In Figure 4a one can see that the system shows no irregular vibrations over a large range of low frequencies of excitation. Over $\omega_0 \approx 6 \text{ N}\cdot\text{m}$, a clear line appears above which the system transits to chaotic behavior. Presented bifurcational diagram (see Figure 4b) shows that in spite of the quasi-periodic and chaotic dynamics, the wide window of period 2 oscillations occurs for $\Omega \in (3,6)$.

Similar observations can be made on the remaining pairs of images representing the results of calculations for higher values of excitation amplitude q . Among others, for $q = 5 \text{ N}\cdot\text{m}$ system passes through a number of states of the multiple period, quasi-periodic and chaotic regions.

4. Conclusions

The present paper is an extension of the work published in reference [18], where a basic nonlinear dynamic analysis and the announcement of the experimental rig has been introduced. In comparison to the previous paper, here we have applied novel techniques for monitoring of the system dynamics by studying nonlinear behaviour maps (number of periods maps), as well as the application of the wavelets transformation techniques, which have been adapted and compared with the standard FFT methods.

The application of Continuous Wavelet Analysis to the investigation of chaotic vibrations of the pendulums is a helpful tool to show and analyse systems behaviour vs. time including a bifurcation diagrams vs. control parameter. The most important role in this type of investigation plays the choice of the proper wavelet base function. The carried out tests and validation approves indicated a Morlet wavelet as the best choice, which is confirmed by research devoted to ([12], [15], [19], [20]).

In conclusion, it was noticed that the double system of physical pendulums despite the small initial deflections (about 0.001 rad) shows an irregular behaviour at relatively low angular velocities. In that conditions, we have been recorded numerous ranges of control parameters for which the vibration character was periodic or quasi-periodic. These test conditions are important from the experimental point of view. Chaotic behaviour obtained from the simulation on a real system is dangerous, since test stand exhibiting chaos can be quickly damaged due to large amplitudes of vibrations.

The developed model brought a good tool for analysis and prediction of nonlinear dynamics of the presented in the previous work real pendulum. That will be the subject of a separate paper.

Appendix

Full form of matrices and vectors **M**, **A**, **B**, **R** from equation (3) in *Wolfram Mathematica* notation.

```

M = {
  {1/2 Cos[φ1(t)]2 (2 I11 + I21 + I23 + 2 e12 m1 + e22 m2 + 2 L12 m2 + 4 e2 L1 m2 Cos[θ2(t)] Cos[φ2(t)] + Ia Cos[2 φ2(t)] - e2 L1 m2 Sin[2 φ1(t)] Sin[φ2(t)] + Sin[φ1(t)]2 (I13 + Ib Sin[θ2(t)]2 + Cos[θ2(t)]2 (I23 Cos[φ2(t)]2 + Ic Sin[φ2(t)]2)) - Ia Cos[θ2(t)] Cos[φ1(t)] Sin[φ1(t)] Sin[2 φ2(t)],

  Sin[θ2[t]] (1/2 Cos[θ2(t)] (-I21 + 2 I22 - I23 + e22 m2 + Ia Cos[2 φ2(t)]) Sin[φ1(t)] + Cos[φ2[t]] (e2 L1 m2 Sin[φ1(t)] + Ia Cos[φ1(t)] Sin[φ2(t)])),

  Cos[θ2(t)] Cos[φ2(t)] (e2 L1 m2 Cos[φ1(t)] - Ia Sin[φ1(t)] Sin[φ2(t)]) + Cos[φ1(t)] (Ic Cos[φ2(t)]2 + I23 Sin[φ2(t)]2), Sin[θ2(t)] (Ib Sin[φ1(t)] - e2 L1 m2 Cos[φ1(t)] Sin[φ2(t)]),

  {Sin[θ2(t)] (1/2 Cos[θ2(t)] (-I21 + 2 I22 - I23 + e22 m2 + Ia Cos[2 φ2(t)]) Sin[φ1(t)] + Cos[φ2(t)] (e2 L1 m2 Sin[φ1(t)] + Ia Cos[φ1(t)] Sin[φ2(t)])),

  I12 + e12 m1 + Ib Cos[θ2(t)]2 + 2 e2 L1 m2 Cos[θ2(t)] Cos[φ2(t)] + Cos[φ2(t)]2 (L12 m2 + I23 Sin[θ2(t)]2) + (L12 m2 + Ic Sin[θ2(t)]2) Sin[φ2(t)]2, Ia Cos[φ2(t)] Sin[θ2(t)] Sin[φ2(t)]),

  Ib Cos[θ2(t)] + e2 L1 m2 Cos[φ2(t)], {Cos[θ2(t)] Cos[φ2(t)] (e2 L1 m2 Cos[φ1(t)] - Ia Sin[φ1(t)] Sin[φ2(t)]) + Cos[φ1(t)] (Ic Cos[φ2(t)]2 + I23 Sin[φ2(t)]2),

  Ia Cos[φ2(t)] Sin[θ2(t)] Sin[φ2(t)],

  Ic Cos[φ2(t)]2 + I23 Sin[φ2(t)]2, 0}, {Sin[θ2(t)] (Ib Sin[φ1(t)] - e2 L1 m2 Cos[φ1(t)] Sin[φ2(t)]), Ib Cos[θ2(t)] + e2 L1 m2 Cos[φ2(t)], 0, Ib}

};

A = {
  {0,
  Sin[θ2(t)] (1/2 Cos[θ2(t)] Cos[φ1(t)] (-I21 + 2 I22 - I23 + e22 m2 + Ia Cos[2 φ2(t)]) + Cos[φ2(t)] (e2 L1 m2 Cos[φ1(t)] - Ia Sin[φ1(t)] Sin[φ2(t)])),

  Cos[φ2(t)] Sin[θ2(t)] (-e2 L1 m2 Cos[φ1(t)] + Ia Sin[φ1(t)] Sin[φ2(t)]),

  -e2 L1 m2 Cos[φ1(t)] Cos[φ2(t)] Sin[θ2(t)],

  -2 (Cos[φ1(t)]2 (e2 L1 m2 + Ia Cos[θ2(t)] Cos[φ2(t)]) Sin[φ2(t)] - e2 L1 m2 Cos[θ2(t)]2 Sin[φ1(t)]2 Sin[φ2(t)] - e2 L1 m2 Sin[θ2(t)]2 Sin[φ1(t)]2 Sin[φ2(t)] + Cos[θ2(t)] Cos[φ2(t)] (e2 L1 m2 Sin[2 φ1(t)] - Ia Sin[φ1(t)]2 Sin[φ2(t)])) + 1/2 Cos[φ1(t)] Sin[φ1(t)] (2 I11 - 2 I13 + I21 - I22 + I23 + 2 e12 m1 + L12 m2 + (I22 + (e22 - L12) m2) Cos[2 θ2(t)] + I21 Cos[2 φ2(t)] - I23 Cos[2 φ2(t)] + e22 m2 Cos[2 φ2(t)] + 2 Cos[θ2(t)]2 (L12 m2 - I23 Cos[φ2(t)]2 - Ic Sin[φ2(t)]2)),

  2 Sin[θ2(t)] (1/2 Cos[θ2(t)] (-I21 + 2 I22 - I23 + e22 m2 + Ia Cos[2 φ2(t)]) Sin[φ1(t)]2 + Cos[φ1(t)] Cos[φ2(t)] (-e2 L1 m2 Cos[φ1(t)] + Ia Sin[φ1(t)] Sin[φ2(t)])),

  2 (-Cos[φ1(t)] Cos[φ2(t)] (e2 L1 m2 Sin[θ2(t)]2 Sin[φ1(t)] + Ia Cos[φ1(t)] Sin[φ2(t)]) + Cos[θ2(t)]2 Cos[φ2(t)] Sin[φ1(t)] (-e2 L1 m2 Cos[φ1(t)] + Ia Sin[φ1(t)] Sin[φ2(t)]) - Cos[θ2(t)] Cos[φ1(t)] (Ia Cos[φ2(t)]2 Sin[φ1(t)] + Sin[φ2(t)] (e2 L1 m2 Cos[φ1(t)] - Ia Sin[φ1(t)] Sin[φ2(t)]))),

  Sin[φ1(t)] (-I22 Sin[θ2(t)]2 - e22 m2 Sin[θ2(t)]2 - Cos[φ2(t)]2 (Ic - I23 Sin[θ2(t)]2) - I23 Sin[φ2(t)]2 + I21 Sin[θ2(t)]2 - Sin[φ2(t)]2 + e22 m2 Sin[θ2(t)]2 Sin[φ2(t)]2 + Cos[θ2(t)]2 (Ib - I23 Cos[φ2(t)]2 - Ic Sin[φ2(t)]2)),

  Sin[θ2[t]] (Cos[φ1(t)] (Ib + Ia Cos[2 φ2(t)]) - Ia Cos[θ2(t)] Sin[φ1(t)] Sin[2 φ2(t)]),
}

```

$\cos[\theta_2[t]] ((I_b - I_a \cos[2\varphi_2(t)]) \sin[\varphi_1(t)] - 2e_2 L_1 m_2 \cos[\varphi_1(t)] \sin[\varphi_2(t)]) - I_a \cos[\varphi_1(t)] \sin[2\varphi_2(t)]\},$
 $\{\cos[\varphi_1(t)]^2 (e_2 L_1 m_2 + I_a \cos[\theta_2(t)] \cos[\varphi_2(t)]) \sin[\varphi_2(t)] - e_2 L_1 m_2 \cos[\theta_2(t)]^2 \sin[\varphi_1(t)]^2 \sin[\varphi_2(t)] - e_2 L_1 m_2 \sin[\theta_2(t)]^2 \sin[\varphi_1(t)]^2 \sin[\varphi_2(t)] + \cos[\theta_2(t)] \cos[\varphi_2(t)] (e_2 L_1 m_2 \sin[2\varphi_1(t)] - I_a \sin[\varphi_1(t)]^2 \sin[\varphi_2(t)]) + \frac{1}{2} \cos[\varphi_1(t)] \sin[\varphi_1(t)] (2I_{11} - 2I_{13} + I_{21} - I_{22} + I_{23} + 2e_1^2 m_1 + L_1^2 m_2 + (I_{22} + (e_2^2 - L_1^2) m_2) \cos[2\theta_2(t)] + I_{21} \cos[2\varphi_2(t)] - I_{23} \cos[2\varphi_2(t)] + e_2^2 m_2 \cos[2\varphi_2(t)] + 2 \cos[\theta_2(t)]^2 (L_1^2 m_2 - I_{23} \cos[\varphi_2(t)]^2 - I_c \sin[\varphi_2(t)]^2)),$
 $0,$
 $I_a \cos[\theta_2(t)] \cos[\varphi_2(t)] \sin[\varphi_2(t)],$
 $-e_2 L_1 m_2 \sin[\varphi_2(t)],$
 $0,$
 $\frac{1}{2} \cos[\theta_2(t)]^2 (-I_{21} + 2I_{22} - I_{23} + e_2^2 m_2 + I_a \cos[2\varphi_2(t)] \sin[\varphi_1(t)] + \sin[\varphi_1(t)] (\cos[\varphi_2(t)]^2 (I_c + I_{23} \sin[\theta_2(t)]^2) + I_{23} \sin[\varphi_2(t)]^2 + \sin[\theta_2(t)]^2 (-I_{22} - e_2^2 m_2 + I_c \sin[\varphi_2(t)]^2)) + \cos[\theta_2[t]] (2e_2 L_1 m_2 \cos[\varphi_2(t)] \sin[\varphi_1(t)] + I_a \cos[\varphi_1(t)] \sin[2\varphi_2(t)]),$
 $-\sin[\theta_2(t)] (\cos[\varphi_1(t)] (I_b - I_a \cos[2\varphi_2(t)]) + \sin[\varphi_1(t)] (2e_2 L_1 m_2 \sin[\varphi_2(t)] + I_a \cos[\theta_2(t)] \sin[2\varphi_2(t)])),$
 $2 \sin[\theta_2(t)] (-e_2 L_1 m_2 \cos[\varphi_2(t)] + \cos[\theta_2(t)] (-I_{22} - e_2^2 m_2 + I_{23} \cos[\varphi_2(t)]^2 + I_c \sin[\varphi_2(t)]^2)),$
 $2 (-e_2 L_1 m_2 \cos[\theta_2(t)] + I_a \cos[\varphi_2(t)] \sin[\theta_2(t)]^2) \sin[\varphi_2(t)],$
 $-(I_b - I_a \cos[2\varphi_2(t)]) \sin[\theta_2(t)],$
 $\{\sin[\theta_2(t)] (-\frac{1}{2}) \cos[\theta_2(t)] (-I_{21} + 2I_{22} - I_{23} + e_2^2 m_2 + I_a \cos[2\varphi_2(t)] \sin[\varphi_1(t)]^2 + \cos[\varphi_1(t)] \cos[\varphi_2(t)] (e_2 L_1 m_2 \cos[\varphi_1(t)] - I_a \sin[\varphi_1(t)] \sin[\varphi_2(t)])),$
 $\sin[\theta_2(t)] (e_2 L_1 m_2 \cos[\varphi_2(t)] + \cos[\theta_2(t)] (I_b - I_{23} \cos[\varphi_2(t)]^2 - I_c \sin[\varphi_2(t)]^2)),$
 $0,0,$
 $-(\frac{1}{2}) \cos[\theta_2(t)]^2 (-I_{21} + 2I_{22} - I_{23} + e_2^2 m_2 + I_a \cos[2\varphi_2(t)] \sin[\varphi_1(t)] - \sin[\varphi_1(t)] (\cos[\varphi_2(t)]^2 (I_c + I_{23} \sin[\theta_2(t)]^2) + I_{23} \sin[\varphi_2(t)]^2 + \sin[\theta_2(t)]^2 (-I_{22} - e_2^2 m_2 + I_c \sin[\varphi_2(t)]^2)) - \cos[\theta_2[t]] (2e_2 L_1 m_2 \cos[\varphi_2(t)] \sin[\varphi_1(t)] + I_a \cos[\varphi_1(t)] \sin[2\varphi_2(t)])),$
 $0,$
 $-\cos[\theta_2(t)] (I_b + I_a \cos[2\varphi_2(t)] \sin[\varphi_1(t)] - I_a \cos[\varphi_1(t)] \sin[2\varphi_2(t)]),$
 $0,$
 $(I_b + I_a \cos[2\varphi_2(t)] \sin[\theta_2(t)],$
 $-I_a \sin[2\varphi_2(t)]\},$
 $\{\cos[\varphi_1(t)] \cos[\varphi_2[t]] (e_2 L_1 m_2 \sin[\theta_2(t)]^2 \sin[\varphi_1(t)] + I_a \cos[\varphi_1(t)] \sin[\varphi_2(t)] + \cos[\theta_2(t)]^2 \cos[\varphi_2(t)] \sin[\varphi_1(t)] (e_2 L_1 m_2 \cos[\varphi_1(t)] - I_a \sin[\varphi_1(t)] \sin[\varphi_2(t)]) + \cos[\theta_2(t)] \cos[\varphi_1(t)] (I_a \cos[\varphi_2(t)]^2 \sin[\varphi_1(t)] + \sin[\varphi_2(t)] (e_2 L_1 m_2 \cos[\varphi_1(t)] - I_a \sin[\varphi_1(t)] \sin[\varphi_2(t)]))),$
 $(e_2 L_1 m_2 \cos[\theta_2(t)] - I_a \cos[\varphi_2(t)] \sin[\theta_2(t)]^2) \sin[\varphi_2(t)],$
 $I_a \cos[\varphi_2(t)] \sin[\varphi_2(t)],$
 $0,$
 $\sin[\theta_2[t]] (\cos[\varphi_1(t)] (I_b - I_a \cos[2\varphi_2(t)]) + \sin[\varphi_1(t)] (2e_2 L_1 m_2 \sin[\varphi_2(t)] + I_a \cos[\theta_2(t)] \sin[2\varphi_2(t)])),$
 $\cos[\theta_2(t)] (I_b + I_a \cos[2\varphi_2(t)] \sin[\varphi_1(t)] + I_a \cos[\varphi_1(t)] \sin[2\varphi_2(t)]),$
 $0,$
 $-(I_b + I_a \cos[2\varphi_2(t)] \sin[\theta_2(t)]),$

$$\begin{aligned}
& 0, \\
& \{0\}; \\
& \mathbf{I} = \{ \\
& \{0, \\
& -\omega (\sin[\theta_1(t)] (\cos[\varphi_1(t)] (-2 e_2 L_1 m_2 \cos[\varphi_2(t)] \sin[\theta_2(t)] + I_{23} \cos[\varphi_2(t)]^2 \sin[2 \theta_2(t)] + \sin[2 \theta_2(t)] (-I_{22} - e_2^2 m_2 + I_a \sin[\theta_2(t)] \sin[\varphi_1(t)] \sin[2 \varphi_2(t)]) + \frac{1}{2} \cos[\theta_1(t)] (\cos[\varphi_1(t)]^2 (2 I_{11} - 2 I_{13} + I_{21} - I_{22} + I_{23} + 2 e_1^2 m_1 + L_1^2 m_2 + (I_{22} + (e_2^2 - L_1^2) m_2) \cos[2 \theta_2(t)] + I_a \cos[2 \varphi_2(t)] + 2 \cos[\theta_2(t)]^2 (I_b - 2 e_2 L_1 m_2 \sin[2 \varphi_1(t)] \sin[\varphi_2(t)] + \cos[\varphi_1(t)]^2 (L_1^2 m_2 - I_{23} \cos[\varphi_2(t)]^2 - I_c \sin[\varphi_2(t)]^2) + \sin[\varphi_1(t)]^2 (-L_1^2 m_2 + I_{23} \cos[\varphi_2(t)]^2 + I_c \sin[\varphi_2(t)]^2)) + 2 (I_{12} + e_1^2 m_1 - \cos[\varphi_2(t)]^2 (-L_1^2 m_2 + I_c \sin[\varphi_1(t)]^2 + \sin[\theta_2(t)]^2 (-I_{23} + L_1^2 m_2 \sin[\varphi_1(t)]^2)) - 2 e_2 L_1 m_2 \sin[\theta_2(t)]^2 \sin[2 \varphi_1(t)] \sin[\varphi_2(t)] + L_1^2 m_2 \sin[\varphi_2(t)]^2 + I_{21} \sin[\theta_2(t)]^2 \sin[\varphi_2(t)]^2 + e_2^2 m_2 \sin[\theta_2(t)]^2 \sin[\varphi_2(t)]^2 - \sin[\varphi_1(t)]^2 (I_{11} - I_{13} + e_1^2 m_1 + I_{23} \sin[\varphi_2(t)]^2 - \sin[\theta_2(t)]^2 (I_b - L_1^2 m_2 \sin[\varphi_2(t)]^2))) - 2 \cos[\theta_2(t)] (-4 e_2 L_1 m_2 \cos[\varphi_1(t)] \cos[\varphi_2(t)] + I_a \sin[2 \varphi_1(t)] \sin[2 \varphi_2(t)]))), \\
& \frac{1}{2} \omega (-\frac{1}{2}) (2 I_{21} + 2 I_{23} + 2 e_2^2 m_2 + 2 (I_{21} - 2 I_{22} + I_{23} - e_2^2 m_2) \cos[2 \theta_2(t)] - I_a \cos[2 (\theta_2(t) - \varphi_2(t))] + 2 I_{21} \cos[2 \varphi_2(t)] - 2 I_{23} \cos[2 \varphi_2(t)] + 2 e_2^2 m_2 \cos[2 \varphi_2(t)] - I_{21} \cos[2 (\theta_2(t) + \varphi_2(t))] + I_{23} \cos[2 (\theta_2(t) + \varphi_2(t))] - e_2^2 m_2 \cos[2 (\theta_2(t) + \varphi_2(t))] \sin[\theta_1(t)] \sin[\varphi_1(t)] + \cos[\theta_1(t)] \sin[\theta_2(t)] (\cos[\theta_2(t)] (-I_{21} + 2 I_{22} - I_{23} + e_2^2 m_2 + I_a \cos[2 \varphi_2(t)] \sin[2 \varphi_1(t)] + 4 \cos[\varphi_2(t)] \sin[\varphi_1(t)] (e_2 L_1 m_2 \cos[\varphi_1(t)] - I_a \sin[\varphi_1(t)] \sin[\varphi_2(t)])))), \\
& \omega (\sin[\theta_1(t)] \sin[\theta_2(t)] (\cos[\varphi_1(t)] (I_b + I_a \cos[2 \varphi_2(t)]) - I_a \cos[\theta_2(t)] \sin[\varphi_1(t)] \sin[2 \varphi_2(t)]) + \frac{1}{4} \cos[\theta_1(t)] (-2 \cos[\theta_2(t)] (2 I_{22} + 2 e_2^2 m_2 + I_a \cos[2 (\varphi_1(t) - \varphi_2(t))] - e_2 L_1 m_2 \cos[2 \varphi_1(t) - \varphi_2(t)] + I_{21} \cos[2 (\varphi_1(t) + \varphi_2(t))] - I_{23} \cos[2 (\varphi_1(t) + \varphi_2(t))] + e_2^2 m_2 \cos[2 (\varphi_1(t) + \varphi_2(t))] + e_2 L_1 m_2 \cos[2 \varphi_1(t) + \varphi_2(t)] + \cos[\varphi_2(t)] (-8 e_2 L_1 m_2 \cos[\varphi_1(t)]^2 + I_a (5 + \cos[2 \theta_2(t)]) \sin[2 \varphi_1(t)] \sin[\varphi_2(t)] + I_a \cos[\theta_2(t)]^2 \sin[2 \varphi_1(t)] \sin[2 \varphi_2(t)]))), \\
& \{\omega (\sin[\theta_1(t)] (\cos[\varphi_1(t)] (-2 e_2 L_1 m_2 \cos[\varphi_2(t)] \sin[\theta_2(t)] + I_{23} \cos[\varphi_2(t)]^2 \sin[2 \theta_2(t)] + \sin[2 \theta_2(t)] (-I_{22} - e_2^2 m_2 + I_c \sin[\varphi_2(t)]^2)) + I_a \sin[\theta_2(t)] \sin[\varphi_1(t)] \sin[2 \varphi_2(t)]) + \frac{1}{2} \cos[\theta_1(t)] (\cos[\varphi_1(t)]^2 (2 I_{11} - 2 I_{13} + I_{21} - I_{22} + I_{23} + 2 e_1^2 m_1 + L_1^2 m_2 + (I_{22} + (e_2^2 - L_1^2) m_2) \cos[2 \theta_2(t)] + I_a \cos[2 \varphi_2(t)] + 2 \cos[\theta_2(t)]^2 (I_b - 2 e_2 L_1 m_2 \sin[2 \varphi_1(t)] \sin[\varphi_2(t)] + \cos[\varphi_1(t)]^2 (L_1^2 m_2 - I_{23} \cos[\varphi_2(t)]^2 - I_c \sin[\varphi_2(t)]^2) + \sin[\varphi_1(t)]^2 (-L_1^2 m_2 + I_{23} \cos[\varphi_2(t)]^2 + I_c \sin[\varphi_2(t)]^2)) + 2 (I_{12} + e_1^2 m_1 - \cos[\varphi_2(t)]^2 (-L_1^2 m_2 + I_c \sin[\varphi_1(t)]^2 + \sin[\theta_2(t)]^2 (-I_{23} + L_1^2 m_2 \sin[\varphi_1(t)]^2)) - 2 e_2 L_1 m_2 \sin[\theta_2(t)]^2 \sin[2 \varphi_1(t)] \sin[\varphi_2(t)] + L_1^2 m_2 \sin[\varphi_2(t)]^2 + I_{21} \sin[\theta_2(t)]^2 \sin[\varphi_2(t)]^2 + e_2^2 m_2 \sin[\theta_2(t)]^2 \sin[\varphi_2(t)]^2 - \sin[\varphi_1(t)]^2 (I_{11} - I_{13} + e_1^2 m_1 + I_{23} \sin[\varphi_2(t)]^2 - \sin[\theta_2(t)]^2 (I_b - L_1^2 m_2 \sin[\varphi_2(t)]^2))) - 2 \cos[\theta_2(t)] (-4 e_2 L_1 m_2 \cos[\varphi_1(t)] \cos[\varphi_2(t)] + I_a \sin[2 \varphi_1(t)] \sin[2 \varphi_2(t)]))), \\
& 0, \\
& \frac{1}{4} \omega (-2 (-2 (I_{21} - 2 I_{22} + I_{23} - e_2^2 m_2) \cos[\theta_2(t)] + I_a \cos[\theta_2(t) - 2 \varphi_2(t)] + 4 e_2 L_1 m_2 \cos[\varphi_2(t)] + I_{21} \cos[\theta_2(t) + 2 \varphi_2(t)] - I_{23} \cos[\theta_2(t) + 2 \varphi_2(t)] + e_2^2 m_2 \cos[\theta_2(t) + 2 \varphi_2(t)]) \sin[\theta_1(t)] \sin[\theta_2(t)] + \cos[\theta_1(t)] (\cos[\varphi_1(t)] (2 I_{21} + 2 I_{23} + 2 e_2^2 m_2 - 2 (I_{21} - 2 I_{22} + I_{23} - e_2^2 m_2) \cos[2 \theta_2(t)] + 4 e_2 L_1 m_2 \cos[\theta_2(t) - \varphi_2(t)] + I_{21} \cos[2 (\theta_2(t) - \varphi_2(t))] - I_{23} \cos[2 (\theta_2(t) - \varphi_2(t))] + e_2^2 m_2 \cos[2 (\theta_2(t) - \varphi_2(t))] + 2 I_{21} \cos[2 \varphi_2(t)] - 2 I_{23} \cos[2 \varphi_2(t)] + 2 e_2^2 m_2 \cos[2 \varphi_2(t)] + 4 e_2 L_1 m_2 \cos[\theta_2(t) + \varphi_2(t)] + I_{21} \cos[2 (\theta_2(t) + \varphi_2(t))] - I_{23} \cos[2 (\theta_2(t) + \varphi_2(t))] + e_2^2 m_2 \cos[2 (\theta_2(t) + \varphi_2(t))] - 4 I_a \cos[\theta_2(t)] \sin[\varphi_1(t)] \sin[2 \varphi_2(t)]))), \\
& \omega (-\frac{1}{2}) (4 e_2 L_1 m_2 \cos[\theta_2(t)] + 2 I_a \cos[\theta_2(t)]^2 \cos[\varphi_2(t)] + I_a (-3 + \cos[2 \theta_2(t)]) \cos[\varphi_2(t)] \sin[\theta_1(t)] \sin[\varphi_2(t)] + \cos[\theta_1(t)] \sin[\theta_2(t)] ((I_b - I_a \cos[2 \varphi_2(t)]) \sin[\varphi_1(t)] - \cos[\varphi_1(t)] (2 e_2 L_1 m_2 \sin[\varphi_2(t)] + I_a \cos[\theta_2(t)] \sin[2 \varphi_2(t)]))), \\
& \{1/2 \omega (\frac{1}{2} (2 I_{21} + 2 I_{23} + 2 e_2^2 m_2 + 2 (I_{21} - 2 I_{22} + I_{23} - e_2^2 m_2) \cos[2 \theta_2(t)] - I_a \cos[2 (\theta_2(t) - \varphi_2(t))] + 2 I_{21} \cos[2 \varphi_2(t)] - 2 I_{23} \cos[2 \varphi_2(t)] + 2 e_2^2 m_2 \cos[2 \varphi_2(t)] - I_{21} \cos[2 (\theta_2(t) + \varphi_2(t))] + I_{23} \cos[2 (\theta_2(t) + \varphi_2(t))] - e_2^2 m_2 \cos[2 (\theta_2(t) + \varphi_2(t))] \sin[\theta_1(t)] \sin[\varphi_1(t)] + \cos[\theta_1(t)] \sin[\theta_2(t)] \sin[\varphi_2(t)] (-\cos[\theta_2(t)] (-I_{21} + 2 I_{22} - I_{23} + e_2^2 m_2 + I_a \cos[2 \varphi_2(t)] \sin[2 \varphi_1(t)] + 4 \cos[\varphi_2(t)] \sin[\varphi_1(t)] (-e_2 L_1 m_2 \cos[\varphi_1(t)] + I_a \sin[\varphi_1(t)] \sin[\varphi_2(t)]))), \\
\end{aligned}$$

$$\begin{aligned}
& -(1/4) \omega (-2 (-2 (I_{21} - 2 I_{22} + I_{23} - e_2^2 m_2) \cos[\theta_2(t)] + I_a \cos[\theta_2(t) - 2 \varphi_2(t)] + 4 e_2 L_1 m_2 \cos[\varphi_2(t)] + I_{21} \cos[\theta_2(t) \\
& + 2 \varphi_2(t)] - I_{23} \cos[\theta_2(t) + 2 \varphi_2(t)] + e_2^2 m_2 \cos[\theta_2(t) + 2 \varphi_2(t)] \sin[\theta_1(t)] \sin[\theta_2(t)] + \cos[\theta_1(t)] (\cos[\varphi_1(t)] (2 \\
& I_{21} + 2 I_{23} + 2 e_2^2 m_2 - 2 (I_{21} - 2 I_{22} + I_{23} - e_2^2 m_2) \cos[2 \theta_2(t)] + 4 e_2 L_1 m_2 \cos[\theta_2(t) - \varphi_2(t)] + I_{21} \cos[2 (\theta_2(t) - \\
& \varphi_2(t))] - I_{23} \cos[2 (\theta_2(t) - \varphi_2(t))] + e_2^2 m_2 \cos[2 (\theta_2(t) - \varphi_2(t))] + 2 I_{21} \cos[2 \varphi_2(t)] - 2 I_{23} \cos[2 \varphi_2(t)] + 2 e_2^2 m_2 \\
& \cos[2 \varphi_2(t)] + 4 e_2 L_1 m_2 \cos[\theta_2(t) + \varphi_2(t)] + I_{21} \cos[2 (\theta_2(t) + \varphi_2(t))] - I_{23} \cos[2 (\theta_2(t) + \varphi_2(t))] + e_2^2 m_2 \cos[2 \\
& (\theta_2(t) + \varphi_2(t))]) - 4 I_a \cos[\theta_2(t)] \sin[\varphi_1(t)] \sin[2 \varphi_2(t)])), \\
& 0, \\
& \omega ((I_b + I_a \cos[2 \varphi_2(t)] \sin[\theta_1(t)] \sin[\theta_2(t)] - \cos[\theta_1(t)] (\cos[\theta_2(t)] \cos[\varphi_1(t)] (I_b + I_a \cos[2 \varphi_2(t)] - I_a \sin[\varphi_1(t)] \\
& \sin[2 \varphi_2(t)]))), \\
& \{\omega (-\sin[\theta_1(t)] \sin[\theta_2(t)] (\cos[\varphi_1(t)] (I_b + I_a \cos[2 \varphi_2(t)]) - I_a \cos[\theta_2(t)] \sin[\varphi_1(t)] \sin[2 \varphi_2(t)]) + 1/4 \cos[\theta_1(t)] \\
& (2 \cos[\theta_2(t)] (2 I_{22} + 2 e_2^2 m_2 + I_a \cos[2 (\varphi_1(t) - \varphi_2(t))] - e_2 L_1 m_2 \cos[2 \varphi_1(t) - \varphi_2(t)] + I_{21} \cos[2 (\varphi_1(t) + \varphi_2(t))] \\
& - I_{23} \cos[2 (\varphi_1(t) + \varphi_2(t))] + e_2^2 m_2 \cos[2 (\varphi_1(t) + \varphi_2(t))] + e_2 L_1 m_2 \cos[2 \varphi_1(t) + \varphi_2(t)] - \cos[\varphi_2(t)] (-8 e_2 L_1 m_2 \\
& \cos[\varphi_1(t)]^2 + I_a (5 + \cos[2 \theta_2(t)] \sin[2 \varphi_1(t)] \sin[\varphi_2(t)]) - I_a \cos[\theta_2(t)]^2 \sin[2 \varphi_1(t)] \sin[2 \varphi_2(t)])), \\
& -\omega (-1/2) (4 e_2 L_1 m_2 \cos[\theta_2(t)] + 2 I_a \cos[\theta_2(t)]^2 \cos[\varphi_2(t)] + I_a (-3 + \cos[2 \theta_2(t)] \cos[\varphi_2(t)] \sin[\theta_1(t)] \\
& \sin[\varphi_2(t)] + \cos[\theta_1(t)] \sin[\theta_2(t)] (I_b - I_a \cos[2 \varphi_2(t)] \sin[\varphi_1(t)] - \cos[\varphi_1(t)] (2 e_2 L_1 m_2 \sin[\varphi_2(t)] + I_a \\
& \cos[\theta_2(t)] \sin[2 \varphi_2(t)]))), \\
& \omega (-I_b + I_a \cos[2 \varphi_2(t)] \sin[\theta_1(t)] \sin[\theta_2(t)] + \cos[\theta_1(t)] (\cos[\theta_2(t)] \cos[\varphi_1(t)] (I_b + I_a \cos[2 \varphi_2(t)] - I_a \\
& \sin[\varphi_1(t)] \sin[2 \varphi_2(t)])), \\
& 0\} \\
& \}; \\
\mathbf{R} = \{ \\
& 1/8 (2 I_{11} \omega^2 \sin[2 \theta_1(t)] - 4 I_{12} \omega^2 \sin[2 \theta_1(t)] + 2 I_{13} \omega^2 \sin[2 \theta_1(t)] - I_{22} \omega^2 \sin[2 \theta_1(t)] - 2 e_1^2 m_1 \omega^2 \sin[2 \theta_1(t)] - \\
& 2 L_1^2 m_2 \omega^2 \sin[2 \theta_1(t)] - 3 I_{22} \omega^2 \cos[\theta_2(t)]^2 \sin[2 \theta_1(t)] - 4 e_2 L_1 m_2 \omega^2 \cos[\theta_2(t)] \cos[\varphi_2(t)] \sin[2 \theta_1(t)] + 3 I_{22} \\
& \omega^2 \sin[2 \theta_1(t)] \sin[\theta_2(t)]^2 + 1/4 \cos[\theta_1(t)] (-\omega^2 (-4 I_{21} - 4 I_{23} + 4 e_2^2 m_2 - 12 (I_{21} + I_{23} - e_2^2 m_2) \cos[2 \theta_2(t)] - 2 \\
& (I_{21} + I_{23} - e_2^2 m_2) \cos[2 (\theta_2(t) - \varphi_1(t))] + 4 I_{21} \cos[2 \varphi_1(t)] + 4 I_{23} \cos[2 \varphi_1(t)] - 4 e_2^2 m_2 \cos[2 \varphi_1(t)] - 2 I_{21} \\
& \cos[2 (\theta_2(t) + \varphi_1(t))] - 2 I_{23} \cos[2 (\theta_2(t) + \varphi_1(t))] + 2 e_2^2 m_2 \cos[2 (\theta_2(t) + \varphi_1(t))] + 6 I_{21} \cos[2 (\theta_2(t) - \varphi_2(t))] - \\
& 6 I_{23} \cos[2 (\theta_2(t) - \varphi_2(t))] + 6 e_2^2 m_2 \cos[2 (\theta_2(t) - \varphi_2(t))] + I_{21} \cos[2 (\theta_2(t) - \varphi_1(t) - \varphi_2(t))] - I_{23} \cos[2 (\theta_2(t) - \\
& \varphi_1(t) - \varphi_2(t))] + e_2^2 m_2 \cos[2 (\theta_2(t) - \varphi_1(t) - \varphi_2(t))] + 6 I_{21} \cos[2 (\varphi_1(t) - \varphi_2(t))] - 6 I_{23} \cos[2 (\varphi_1(t) - \varphi_2(t))] + 6 \\
& e_2^2 m_2 \cos[2 (\varphi_1(t) - \varphi_2(t))] + I_{21} \cos[2 (\theta_2(t) + \varphi_1(t) - \varphi_2(t))] - I_{23} \cos[2 (\theta_2(t) + \varphi_1(t) - \varphi_2(t))] + e_2^2 m_2 \cos[2 \\
& (\theta_2(t) + \varphi_1(t) - \varphi_2(t))] - 12 I_{21} \cos[2 \varphi_2(t)] + 12 I_{23} \cos[2 \varphi_2(t)] - 12 e_2^2 m_2 \cos[2 \varphi_2(t)] + 6 I_{21} \cos[2 (\theta_2(t) + \\
& \varphi_2(t))] - 6 I_{23} \cos[2 (\theta_2(t) + \varphi_2(t))] + 6 e_2^2 m_2 \cos[2 (\theta_2(t) + \varphi_2(t))] + I_{21} \cos[2 (\theta_2(t) - \varphi_1(t) + \varphi_2(t))] - I_{23} \cos[2 \\
& (\theta_2(t) - \varphi_1(t) + \varphi_2(t))] + e_2^2 m_2 \cos[2 (\theta_2(t) - \varphi_1(t) + \varphi_2(t))] + 6 I_{21} \cos[2 (\varphi_1(t) + \varphi_2(t))] - 6 I_{23} \cos[2 (\varphi_1(t) + \\
& \varphi_2(t))] + 6 e_2^2 m_2 \cos[2 (\varphi_1(t) + \varphi_2(t))] + I_{21} \cos[2 (\theta_2(t) + \varphi_1(t) + \varphi_2(t))] - I_{23} \cos[2 (\theta_2(t) + \varphi_1(t) + \varphi_2(t))] + e_2^2 \\
& m_2 \cos[2 (\theta_2(t) + \varphi_1(t) + \varphi_2(t))] \sin[\theta_1(t)] + 32 e_2 g m_2 \cos[\varphi_2(t)] \sin[\theta_2(t)] - \omega^2 \cos[\varphi_1(t)]^2 \sin[2 \theta_1(t)] (2 I_{11} \\
& - 2 I_{13} - I_{22} + 2 e_1^2 m_1 + 2 L_1^2 m_2 + I_{22} \cos[\theta_2(t)]^2 + 4 e_2 L_1 m_2 \cos[\theta_2(t)] \cos[\varphi_2(t)] - I_{22} \sin[\theta_2(t)]^2 + 2 I_{11} \omega^2 \\
& \sin[2 \theta_1(t)] \sin[\varphi_1(t)]^2 - 2 I_{13} \omega^2 \sin[2 \theta_1(t)] \sin[\varphi_1(t)]^2 - I_{22} \omega^2 \sin[2 \theta_1(t)] \sin[\varphi_1(t)]^2 + 2 e_1^2 m_1 \omega^2 \sin[2 \theta_1(t)] \\
& \sin[\varphi_1(t)]^2 + 2 L_1^2 m_2 \omega^2 \sin[2 \theta_1(t)] \sin[\varphi_1(t)]^2 + I_{22} \omega^2 \cos[\theta_2(t)]^2 \sin[2 \theta_1(t)] \sin[\varphi_1(t)]^2 + 4 e_2 L_1 m_2 \omega^2 \\
& \cos[\theta_2(t)] \cos[\varphi_2(t)] \sin[2 \theta_1(t)] \sin[\varphi_1(t)]^2 - I_{22} \omega^2 \sin[2 \theta_1(t)] \sin[\theta_2(t)]^2 \sin[\varphi_1(t)]^2 - 8 e_2 g m_2 \sin[\theta_1(t)] \\
& \sin[\varphi_1(t)] \sin[\varphi_2(t)] + 4 e_2 L_1 m_2 \omega^2 \sin[2 \theta_1(t)] \sin[2 \varphi_1(t)] \sin[\varphi_2(t)] + 2 \cos[\varphi_1(t)] \sin[\theta_1(t)] (4 e_1 g m_1 + 4 g \\
& L_1 m_2 + 4 e_2 g m_2 \cos[\theta_2(t)] \cos[\varphi_2(t)] + 4 e_2 L_1 m_2 \omega^2 \cos[\varphi_2(t)] \sin[\theta_1(t)] \sin[\theta_2(t)] - I_{21} \omega^2 \sin[\theta_1(t)] \sin[2 \\
& \theta_2(t)] + 2 I_{22} \omega^2 \sin[\theta_1(t)] \sin[2 \theta_2(t)] - I_{23} \omega^2 \sin[\theta_1(t)] \sin[2 \theta_2(t)] + e_2^2 m_2 \omega^2 \sin[\theta_1(t)] \sin[2 \theta_2(t)] + I_a \omega^2 \\
& \cos[\varphi_2(t)]^2 \sin[\theta_1(t)] \sin[2 \theta_2(t)] - I_{21} \omega^2 \sin[\theta_1(t)] \sin[2 \theta_2(t)] \sin[\varphi_2(t)]^2 + I_{23} \omega^2 \sin[\theta_1(t)] \sin[2 \theta_2(t)] \\
& \sin[\varphi_2(t)]^2 - e_2^2 m_2 \omega^2 \sin[\theta_1(t)] \sin[2 \theta_2(t)] \sin[\varphi_2(t)]^2 - 4 I_{21} \omega^2 \sin[\theta_1(t)]^2 \sin[\theta_2(t)] \sin[\varphi_1(t)] \sin[2 \varphi_2(t)] + \\
& 4 I_{23} \omega^2 \sin[\theta_1(t)]^2 \sin[\theta_2(t)] \sin[\varphi_1(t)] \sin[2 \varphi_2(t)] - 4 e_2^2 m_2 \omega^2 \sin[\theta_1(t)]^2 \sin[\theta_2(t)] \sin[\varphi_1(t)] \sin[2 \varphi_2(t)] + 2
\end{aligned}$$

$$I_{21} \omega^2 \cos[\theta_2(t)] \sin[2 \theta_1(t)] \sin[2 \varphi_1(t)] \sin[2 \varphi_2(t)] - 2 I_{23} \omega^2 \cos[\theta_2(t)] \sin[2 \theta_1(t)] \sin[2 \varphi_1(t)] \sin[2 \varphi_2(t)] + 2 e_2^2 m_2 \omega^2 \cos[\theta_2(t)] \sin[2 \theta_1(t)] \sin[2 \varphi_1(t)] \sin[2 \varphi_2(t)] - 4 \omega^2 \cos[\theta_1(t)]^2 \sin[\theta_2(t)] (\cos[\varphi_1(t)] (2 e_2 L_1 m_2 \cos[\varphi_2(t)] + \cos[\theta_2(t)] (-I_{21} + 2 I_{22} - I_{23} + e_2^2 m_2 + I_a \cos[2 \varphi_2(t)])) - I_a \sin[\varphi_1(t)] \sin[2 \varphi_2(t)])),$$

$$\begin{aligned} & 1/8 (8 g \cos[\theta_1(t)] ((e_1 m_1 + L_1 m_2 + e_2 m_2 \cos[\theta_2(t)] \cos[\varphi_2(t)]) \sin[\varphi_1(t)] + e_2 m_2 \cos[\varphi_1(t)] \sin[\varphi_2(t)]) - 1/4 \omega^2 \\ & \cos[\theta_1(t)]^2 ((8 I_{11} - 8 I_{13} + 2 I_{21} - 4 I_{22} + 2 I_{23} + 8 e_1^2 m_1 - 2 e_2^2 m_2 + 8 L_1^2 m_2 + 4 I_{22} \cos[\theta_2(t)]^2 - 2 (I_{21} + I_{23} - e_2^2 m_2) \cos[2 \theta_2(t)] + I_{21} \cos[2 (\theta_2(t) - \varphi_2(t))] - I_{23} \cos[2 (\theta_2(t) - \varphi_2(t))] + e_2^2 m_2 \cos[2 (\theta_2(t) - \varphi_2(t))] + 16 e_2 L_1 m_2 \cos[\theta_2(t)] \cos[\varphi_2(t)] + 6 I_{21} \cos[2 \varphi_2(t)] - 6 I_{23} \cos[2 \varphi_2(t)] + 6 e_2^2 m_2 \cos[2 \varphi_2(t)] + I_{21} \cos[2 (\theta_2(t) + \varphi_2(t))] - I_{23} \cos[2 (\theta_2(t) + \varphi_2(t))] + e_2^2 m_2 \cos[2 (\theta_2(t) + \varphi_2(t))] - 4 I_{22} \sin[\theta_2(t)]^2) \sin[2 \varphi_1(t)] + 8 \cos[2 \varphi_1(t)] (2 e_2 L_1 m_2 \sin[\varphi_2(t)] + I_a \cos[\theta_2(t)] \sin[2 \varphi_2(t)])) - 1/2 \omega^2 (\cos[\theta_1(t)]^2 (I_a \cos[2 \theta_2(t)] \cos[2 \varphi_2(t)] \sin[2 \varphi_1(t)] + (I_{21} + I_{23} - e_2^2 m_2 - (I_{21} + I_{23} - e_2^2 m_2) \cos[2 \theta_2(t)] + 3 I_a \cos[2 \varphi_2(t)])) \sin[2 \varphi_1(t)] + 4 \cos[\varphi_1(t)]^2 (2 e_2 L_1 m_2 \sin[\varphi_2(t)] + I_a \cos[\theta_2(t)] \sin[2 \varphi_2(t)])) - 2 (I_a \cos[\varphi_2(t)]^2 \sin[2 \theta_1(t)] \sin[2 \theta_2(t)] \sin[\varphi_1(t)] + 4 e_2 L_1 m_2 \cos[\varphi_2(t)] (\sin[2 \theta_1(t)] \sin[\theta_2(t)] \sin[\varphi_1(t)] - \cos[\theta_1(t)]^2 \cos[\theta_2(t)] \sin[2 \varphi_1(t)]) + 1/2 \sin[2 \theta_1(t)] ((-3 I_{21} + 4 I_{22} - I_{23} + e_2^2 m_2 + I_a \cos[2 \varphi_2(t)] \sin[2 \theta_2(t)] + 4 I_a \cos[\varphi_1(t)] \sin[\theta_2(t)] \sin[2 \varphi_2(t)] - \cos[\theta_1(t)]^2 ((2 I_{11} - 2 I_{13} - I_{22} + 2 e_1^2 m_1 + 2 L_1^2 m_2 + I_{22} \cos[2 \theta_2(t)])) \sin[2 \varphi_1(t)] - 2 \sin[\varphi_1(t)]^2 (2 e_2 L_1 m_2 \sin[\varphi_2(t)] + I_a \cos[\theta_2(t)] \sin[2 \varphi_2(t)]))))), \end{aligned}$$

$$\begin{aligned} & 1/8 (-2 \omega^2 \cos[\theta_2(t)]^2 \cos[\varphi_1(t)] (-I_{21} + 2 I_{22} - I_{23} + e_2^2 m_2 + I_a \cos[2 \varphi_2(t)])) \sin[2 \theta_1(t)] - e_2 m_2 (-6 L_1 \omega^2 + 2 L_1 \omega^2 \\ & \cos[2 \theta_1(t)] - 4 g \cos[\theta_1(t) - \varphi_1(t)] + L_1 \omega^2 \cos[2 (\theta_1(t) - \varphi_1(t))] + 2 L_1 \omega^2 \cos[2 \varphi_1(t)] - 4 g \cos[\theta_1(t) + \varphi_1(t)] + L_1 \omega^2 \cos[2 (\theta_1(t) + \varphi_1(t))] \cos[\varphi_2(t)] \sin[\theta_2(t)] + 2 I_a \omega^2 \cos[\varphi_1(t)] \cos[\varphi_2(t)]^2 \sin[2 \theta_1(t)] \sin[\theta_2(t)]^2 + \omega^2 (\cos[\varphi_1(t)] (-3 I_{21} + 4 I_{22} - I_{23} + e_2^2 m_2 + I_a \cos[2 \varphi_2(t)])) \sin[2 \theta_1(t)] \sin[\theta_2(t)]^2 - 2 I_{22} \cos[\theta_1(t)]^2 \cos[\varphi_1(t)]^2 \sin[2 \theta_2(t)] - 1/4 I_{22} (-6 + 10 \cos[2 \theta_1(t)] + \cos[2 (\theta_1(t) - \varphi_1(t))] + 2 \cos[2 \varphi_1(t)] + \cos[2 (\theta_1(t) + \varphi_1(t))] \sin[2 \theta_2(t)] + 2 I_a \cos[\theta_1(t)] \sin[2 \varphi_1(t)] \sin[2 \varphi_2(t)] + \cos[\theta_1(t)] (4 e_2 m_2 \cos[\varphi_2(t)] (2 g \sin[\theta_1(t)] - L_1 \omega^2 \cos[\varphi_1(t)] \sin[2 \theta_1(t)]) - 1/2 I_a \omega^2 (-2 + 6 \cos[2 \theta_1(t)] + \cos[2 (\theta_1(t) - \varphi_1(t))] + 2 \cos[2 \varphi_1(t)] + \cos[2 (\theta_1(t) + \varphi_1(t))] \cos[\varphi_2(t)]^2 \sin[\theta_2(t)] + \omega^2 (-1/4) (-2 + 6 \cos[2 \theta_1(t)] + \cos[2 (\theta_1(t) - \varphi_1(t))] + 2 \cos[2 \varphi_1(t)] + \cos[2 (\theta_1(t) + \varphi_1(t))]) (-3 I_a + I_a \cos[2 \varphi_2(t)])) \sin[\theta_2(t)] + 2 I_a \sin[2 \theta_1(t)] \sin[\varphi_1(t)] \sin[2 \varphi_2(t)]))), \end{aligned}$$

$$\begin{aligned} & 1/8 (-4 I_a \omega^2 \cos[\theta_1(t)] \cos[\varphi_2(t)]^2 (\cos[\theta_1(t)] \cos[\theta_2(t)] \cos[\varphi_1(t)] - 2 \sin[\theta_1(t)] \sin[\theta_2(t)] \sin[\varphi_1(t)] + 8 e_2 g m_2 \cos[\theta_1(t)] (\cos[\varphi_2(t)] \sin[\varphi_1(t)] + \cos[\theta_2(t)] \cos[\varphi_1(t)] \sin[\varphi_2(t)]) + \omega^2 \cos[\varphi_2(t)] (-2 e_2 L_1 m_2 \cos[\theta_1(t)]^2 \sin[2 \varphi_1(t)] - 1/8 I_a (20 - 12 \cos[2 \theta_1(t)] + 6 \cos[2 (\theta_1(t) - \theta_2(t))] - 20 \cos[2 \theta_2(t)] + 6 \cos[2 (\theta_1(t) + \theta_2(t))] + 6 \cos[2 (\theta_1(t) - \varphi_1(t))] + \cos[2 (\theta_1(t) - \theta_2(t) - \varphi_1(t))] + 2 \cos[2 (\theta_2(t) - \varphi_1(t))] + \cos[2 (\theta_1(t) + \theta_2(t) - \varphi_1(t))] + 12 \cos[2 \varphi_1(t)] + 6 \cos[2 (\theta_1(t) + \varphi_1(t))] + \cos[2 (\theta_1(t) - \theta_2(t) + \varphi_1(t))] + 2 \cos[2 (\theta_2(t) + \varphi_1(t))] + \cos[2 (\theta_1(t) + \theta_2(t) + \varphi_1(t))] \sin[\varphi_2(t)] + \omega^2 \cos[\theta_1(t)]^2 (-2 I_a \cos[\theta_2(t)] \cos[\varphi_2(t)]^2 \sin[2 \varphi_1(t)] + \cos[\varphi_2(t)] (-2 e_2 L_1 m_2 \sin[2 \varphi_1(t)] - 1/2 I_a (-6 + 6 \cos[2 \theta_2(t)] + \cos[2 (\theta_2(t) - \varphi_1(t))] + 6 \cos[2 \varphi_1(t)] + \cos[2 (\theta_2(t) + \varphi_1(t))] \sin[\varphi_2(t)] + 4 \cos[\theta_2(t)] \cos[\varphi_1(t)] \sin[\varphi_2(t)] (-e_2 L_1 m_2 \cos[\varphi_1(t)] + I_a \sin[\varphi_1(t)] \sin[\varphi_2(t)])) - 2 (4 e_2 g m_2 \sin[\theta_1(t)] \sin[\theta_2(t)] \sin[\varphi_2(t)] + \omega^2 \cos[\theta_2(t)] \sin[\varphi_2(t)] (-3 e_2 L_1 m_2 + e_2 L_1 m_2 \cos[\theta_1(t)]^2 \cos[\varphi_1(t)]^2 - e_2 L_1 m_2 \sin[\varphi_1(t)]^2 - I_{21} \sin[2 \varphi_1(t)] \sin[\varphi_2(t)] + I_{23} \sin[2 \varphi_1(t)] \sin[\varphi_2(t)] - e_2^2 m_2 \sin[2 \varphi_1(t)] \sin[\varphi_2(t)] + \sin[\theta_1(t)]^2 (-e_2 L_1 m_2 + e_2 L_1 m_2 \sin[\varphi_1(t)]^2 + I_a \sin[2 \varphi_1(t)] \sin[\varphi_2(t)])) - \omega^2 \sin[2 \theta_1(t)] (-2 I_a \sin[\theta_2(t)] \sin[\varphi_1(t)] \sin[\varphi_2(t)]^2 + \cos[\varphi_1(t)] (2 e_2 L_1 m_2 \sin[\theta_2(t)] \sin[\varphi_2(t)] + I_a \sin[2 \theta_2(t)] \sin[2 \varphi_2(t)]))))), \end{aligned}$$

where

$$I_a = I_{21} - I_{23} + e_2^2 m_2,$$

$$I_b = I_{22} + e_2^2 m_2,$$

$$I_c = I_{21} + e_2^2 m_2.$$

Acknowledgments

This paper was financially supported by the National Science Centre of Poland under the grant MAESTRO 2, No. 2012/04/A/ST8/00738, for years 2013-2016.

References

1. J. Shen, A. K. Sanyal, N. A. Chaturvedi, D. Bernstein, H. McClamroch. Dynamics and control of a 3D pendulum. *43rd IEEE Conference on Decision and Control, 2004. CDC 1* (2004), 323–328.
2. N. A. Chaturvedi, N. H. McClamroch. Asymptotic stabilization of the hanging equilibrium manifold of the 3D pendulum. *International Journal of Robust and Nonlinear Control* 17, 16 (2007), 1435–1454.
3. N. A. Chaturvedi, T. Lee, M. Leok, N. H. McClamroch. Nonlinear Dynamics of the 3D Pendulum. *Journal of Nonlinear Science* 21, 1 (2010), 3–32.
4. J. Náprstek, C. Fischer. Types and stability of quasi-periodic response of a spherical pendulum. *Computers & Structures* 124 (2013), 74–87.
5. L. Consolini, M. Tosques. On the exact tracking of the spherical inverted pendulum via an homotopy method. *Systems & Control Letters* 58, 1 (2009), 1–6.
6. I. M. Anan'evskii, N. V. Anokhin. Control of the spatial motion of a multilink inverted pendulum using a torque applied to the first link. *Journal of Applied Mathematics and Mechanics* 78, 6 (2014), 543–550.
7. T. Lee, M. Leok, and N. H. McClamroch, Dynamics and Control of a Chain Pendulum on a Cart. *Proc. of the IEEE Conference on Decision and Control*, (2012), 2502–2508.
8. Xinjilefu, V. Hayward, H. Michalska. Hybrid Stabilizing Control for the Spatial Double Inverted Pendulum. *Brain, Body and Machine*, Springer Berlin Heidelberg, (2010), 201–215.
9. P. Egger and L. Caracoglia. Analytical and experimental investigation on a multiple-mass-element pendulum impact damper for vibration mitigation. *Journal of Sound and Vibration* 353, (2015), 38–57.
10. M. McGrath, D. Howard, R. Baker. The strengths and weaknesses of inverted pendulum models of human walking. *Gait & Posture* 41, 2 (2015), 389–394.
11. H. Ozaki, K. Ohta, and T. Jinji. Multi-body power analysis of kicking motion based on a double pendulum. *Procedia Engineering* 34 (2012), 218–223.
12. J. Awrejcewicz, A. V. Krysko, N. A. Zagniboroda, V. V. Dobriyan, V. A. Krysko. On the general theory of chaotic dynamics of flexible curvilinear Euler–Bernoulli beams. *Nonlinear Dynamics* 79, 1 (2014), 11–29.
13. K. Vernekar, H. Kumar, K. V. Gangadharan. Gear Fault Detection Using Vibration Analysis and Continuous Wavelet Transform. *Procedia Materials Science* 5, (2014), 1846–1852.
14. N. G. Nikolaou, I. A. Antoniadis. Demodulation of vibration signals generated by defects in rolling element bearings using complex shifted Morlet wavelets. *Mechanical Systems and Signal Processing* 16, 4 (2002), 677–694.
15. H. Li, T. Yi, M. Gu, L. Huo. Evaluation of earthquake-induced structural damages by wavelet transform. *Progress in Natural Science* 19, 4 (2009), 461–470.
16. J. Gross. Analytical methods and experimental approaches for electrophysiological studies of brain oscillations. *Journal of Neuroscience Methods* 228, (2014), 57–66.
17. R. Büssow. An algorithm for the continuous Morlet wavelet transform. *Mechanical Systems and Signal Processing* 21, 8 (2007), 2970–2979.
18. M. Ludwicki, J. Awrejcewicz, G. Kudra. Spatial double physical pendulum with axial excitation: computer simulation and experimental set-up. *International Journal of Dynamics and Control* 3, 1 (2014), 1–8.

19. J. Awrejcewicz, A. V. Krysko et al. Analysis of chaotic vibrations of flexible plates using fast Fourier transforms and wavelets. *International Journal of Structural Stability and Dynamics* 13, 7 (2013), 1340005.
20. J. Awrejcewicz et al. Analysis of chaotic vibrations of flexible plates using Fast Fourier Transforms and wavelets. *International Journal of Structural Stability and Dynamics* 13, 7 (2013), 1340005-1 - 1340004-12.

Michał Ludwicki, Ph.D.: Lodz University of Technology, Department of Automation, Biomechanics and Mechatronics, 1/15 Stefanowski St., 90-924 Lodz, Poland (michal.ludwicki@p.lodz.pl). The author gave a presentation of this paper during one of the conference sessions.

Jan Awrejcewicz, Professor: Lodz University of Technology, Department of Automation, Biomechanics and Mechatronics, 1/15 Stefanowski St., 90-924 Lodz, Poland (jan.awrejcewicz@p.lodz.pl).

Grzegorz Kudra, Ph.D.: Lodz University of Technology, Department of Automation, Biomechanics and Mechatronics, 1/15 Stefanowski St., 90-924 Lodz, Poland (grzegorz.kudra@p.lodz.pl).